Journal of Mechanical Engineering and Sciences
ISSN (Print): 2289-4659; e-ISSN: 2231-8380
Volume 13, Issue 3, pp. 5455-5479, September 2019

DOI: https://doi.org/10.15282/jmes.13.3.2019.16.0442

Optimal design of junctionless double gate vertical MOSFET using hybrid Taguchi-GRA with ANN prediction

K. E. Kaharudin[1], F. Salehuddin[1,*], A. S. M. Zain[1] and Ameer F. Roslan[1]

[1]MiNE, CeTRI, Faculty of Electronics and Computer Engineering (FKEKK),
Universiti Teknikal Malaysia Melaka (UTeM), Hang Tuah Jaya,
76100 Durian Tunggal, Melaka, Malaysia.
[*]Email: fauziyah@utem.edu.my
Phone: +6062702361; Fax: +6062701045

ABSTRACT

Random parameter variations have been an influential factor that deciding the performance of a metal-oxide-semiconductor field effect transistor (MOSFET), especially in nano-scale regime. Thus, controlling the variation of those parameters becomes extremely crucial in order to attain an acceptable performance of an ultra-small MOSFET. This paper proposes an approach to optimally design a n-type junctionless double-gate vertical MOSFET (n-JLDGVM) via hybrid Taguchi-grey relational analysis (GRA) with artificial neural networks (ANN) prediction. The device is designed using a combination of 2-D simulation tools (Silvaco) and hybrid Taguchi-GRA with a well-trained ANN prediction. The investigated device parameters consist of channel length (L_{ch}), pillar thickness (T_p), channel doping (N_{ch}) and source/drain doping (N_{sd}). The optimized design parameters of the device demonstrate a tolerable magnitude of on-state current (I_{ON}), off-state current (I_{OFF}), on-off ratio, transconductance (g_m), cut-off frequency (f_T) and maximum oscillation frequency (f_{max}), measured at 2344.9 µA/µm, 2.53 pA/µm, 927 x 10^6, 4.78 mS/µm, 121.5 GHz and 2469 GHz respectively.

Keywords: Channel doping; channel length; pillar thickness; source/drain doping.

INTRODUCTION

For over several decades, the metal-oxide semiconductor field effect transistors (MOSFET) have been continually scaled down. The primary reason behind the aggressive scaling on the MOSFET's dimensions is to allow hundreds of millions of transistors to be integrated in a single chip. The ultra-small MOSFETs increase the functionality and reduce the cost of the integrated circuits which provides a mutual advantage for both end users and chip manufacturers. The MOSFET's scaling offers remarkable advantages for microchip industries such as a low cost of manufacturing, increased speed of data transfer and high frequency applications. Intrinsic parameter fluctuations in a scaled transistor is one of the important factors to be considered for investigating the scaling parameters [1]. According to the latest update of International Technology Roadmap of Semiconductors (ITRS) 2013 report [2], transistors with channel length (L_{ch}) of 10.6 nm are required for the high

performance (HP) logic technology in the year 2020. The variations in L_{ch} do contribute a significant impact on the transistor's characteristics. The random number and position of dopants that reside in the short channel of the silicon lattice would introduce significant variation on the electrical characteristics such as threshold voltage (V_{TH}), drain-to-source current (I_{ds}) on-state current (I_{ON}), off-state current (I_{OFF}) and on-off ratio. Since the I_{ds} is an important parameter used for small-signal analysis of a transistor, the scaling parameter variation would contribute a significant impact on analog and RF properties such as transconductance (g_m), cut-off frequency (f_T) and maximum oscillation frequency (f_{max}). Previous research works have indicated that the variation in L_{ch} and body thickness (T_{body}) have an enormous impact on the electrical characteristics of a transistor [3-7]. Thus, scaling the geometrical parameters such as L_{ch} and T_{body} requires a very careful consideration for better transistor's performance.

The intrinsic parameters fluctuations associated with random dopant distributions have been widely studied by many of electronic researchers and scientists. In the early study conducted by Hoeneison & Mad [8], it was shown that a non-uniform distribution of random dopant in the channel region did cause a mismatch in the V_{TH} of a transistor. The influence of the random dopants on the intrinsic parameters was then analytically studied by Hagowara *et al.* [9] in order to predict the V_{TH} variation via simple mathematical model. Furthermore, the impact of intrinsic parameter fluctuations in V_{TH} has also been comprehensively investigated via a 3-D atomistic simulations by Asenov *et al.* [10-13]. Random dopant distributions that caused by ion implantation processes have become a dominant source of statistical variability in ultra-small scaled transistor technology. Thus, efficient approaches are definitely required to reduce the variability of the design parameters [14]. One of the common approaches used for analyzing the impact of the design parameter variation is known as design of experiment (DoE). Ramakrishnan in his report [1], has conducted a comparative analysis between the efficiency of Monte Carlo analysis and the DoE based on response surface methodology (RSM) in studying the design parameter variation on the V_{TH} for 65nm MOSFETs technology node. The results indicated that the RSM requires less time with simulations compared to Monte Carlo technique in investigating the variability of the design parameters towards the V_{TH} fluctuations. However, the variability analysis performed via RSM was observed to be inefficient when very large number of design parameters were involved due to interaction effects.

Another statistical approach used in optimizing the parameter variation is known as Taguchi method. Several research reports have shown that Taguchi method was capable of optimizing multiple design parameters in various of transistor's structures [15-21]. Taguchi method with its special orthogonal array (OA) offers lesser experiment runs and simpler DoE compared to RSM [22-23], but it is however limited to a single response (electrical characteristic) optimization. Thus, an analytical algorithm which capable of converting multiple responses into a single representative grade, named as grey relational analysis (GRA) is introduced. Through GRA, the multi-objective optimization problems of the design can be possibly solved by using Taguchi method. Several previous reports have proved that the hybrid Taguchi-GRA had a capability to solve multi-objective optimization problems in various engineering fields [24-31]. Although the Taguchi-GRA could optimize multiple responses simultaneously, it is however only capable of addressing discrete design parameters, rather than continuous design parameters. In other words, the Taguchi-GRA is only able to search optimal solutions within the specified level of design parameters. To

compensate this disadvantage, the artificial neural networks (ANN) is introduced to Taguchi-GRA in which it opens the possibility to further predict and tune the design parameters for robust optimization solution [32-34]. This paper describes a proposed method to optimally design a n-type junctionless double-gate vertical MOSFET (n-JLDGVM) via hybrid Taguchi-GRA with artificial neural networks (ANN) prediction. The proposed work in this paper is organized as follows: Section 2 explains the n-JLDGVM device schematic, structure and simulation. Section 3 describes the simultaneous optimization of design parameters towards the I_{ON}, I_{OFF}, on-off ratio, g_m, f_t and f_{max} using Taguchi-GRA. Section 4 describes the application of ANN prediction to further tuning the design parameters for better optimization solution. Finally, section 5 briefly summarizes the conclusions and future work of this study.

DEVICE DIMENSION AND SIMULATION

A 2-D process simulation flow and schematic layout for an ultrathin n-JLDGVM device are shown in Figure 1 and Figure 2 correspondingly. The process simulation was initiated with the main silicon (Si) substrate which was doped with 5 x 10^{18} atom/cm^3 of arsenic dopant. The Si substrate was then etched to form a sharp ultrathin vertical pillar with a thickness of 9nm. The thinning process of the Si-pillar was very important to enable the channel to be fully depleted as a certain gate-to-source voltage (V_{gs}) was applied, thereby modulating the electrical conductivity. High-k/metal-gate (HKMG) deposition was performed in which both sides of the ultrathin pillar were covered by the hafnium dioxide (HfO_2) layer followed by the tungsten silicide (WSi_x) layer. The HKMG process is very crucial to prevent the carriers mobility degradation due to phonon scattering and Fermi level pinning [35-36].

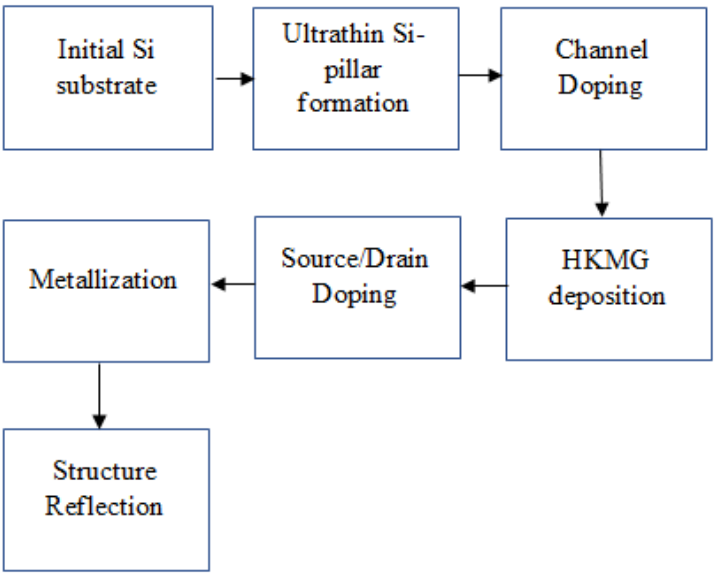

Figure 1. Process flow for ultra-thin n-JLDGVM device.

The metal work function for the WSi_x layer was tuned at 4.5 eV. Finding the correct work function for the device is very crucial for stabilizing the V_{TH} as well as other electrical

characteristics. The source/drain (S/D) region was then doped with 5 x 10^{18} atom/cm^3 of arsenic dopant. The same dopant type (Arsenic) was applied to both channel and S/D region in order to form N N^+ N (junctionless) configuration. Thus, the adversity of forming the intricate junction for short channel device can be totally neglected as the current conduction in junctionless device was governed by bulk transport phenomenon and high channel doping (N_{ch}) concentration. The metallization process was then performed and any unwanted aluminum was etched for source/drain and gate formation.

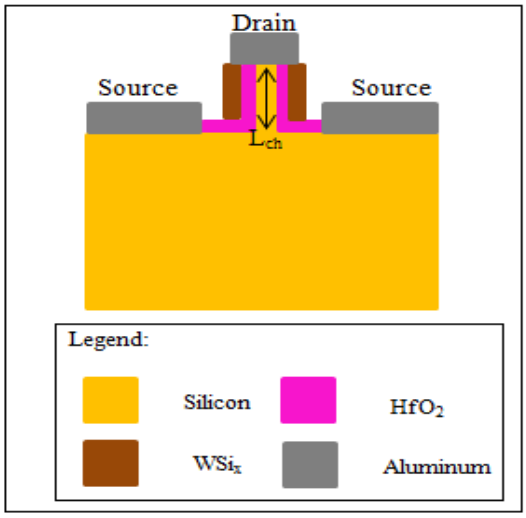

Figure 2. 2-D cross-section of the n-JLDGVM device.

Finally, the structure was reflected in both x and y axis to form a complete n-JLSDGM structure as depicted in Figure 3. The initial design parameters used for simulating the device are shown in Table 1.

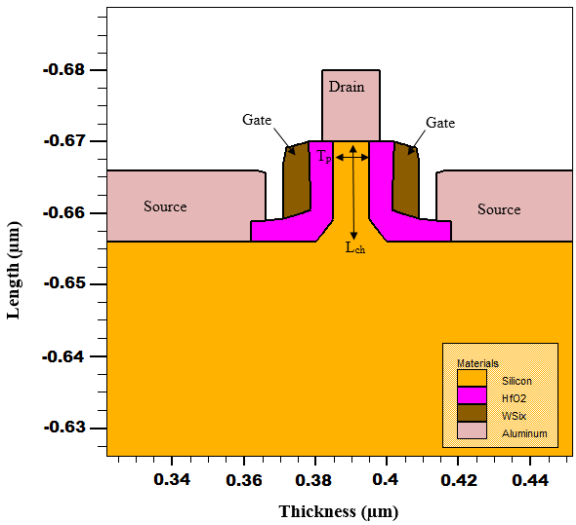

Figure 3. 2-D cross-section of the n-JLDGVM device.

Table 1. Initial design parameters of n-JLDGVM device.

Design Parameters	Units	Initial Value
Channel Length, L_{ch}	nm	10
Pillar Thickness, L_p	nm	9
Channel doping, N_{ch}	Atom/cm^3	5.0 x 10^{18}
S/D doping, N_{sd}	Atom/cm^3	5.0 x 10^{18}

The n-JLDGVM device was then simulated via Atlas Silvaco module for extracting the electrical characteristics. In this study, the drain-to-source voltage (V_{ds}) was supplied at a constant value of 0.5V while the gate-to-source voltage (V_{gs}) was varied from 0V to 1V. The device simulation involved both DC and small signal analysis in order to extract and compute the electrostatic, analog and RF characteristics of the device. The device simulation was based on the Lombardi CVT and temperature mobility model for accurate prediction of the behaviors of the n-JLDGVM device. The impact of high surface scattering that might cause the mobility degradation would be well considered by using these models. Apart from that, the Shockley-Read-Hall Recombination (SRH) model was applied in order to consider the impact of phonon transition effects on the leakage attribute of the device. Since the channel of the device was extremely thin, the quantum effects were considered by employing quantum drift-diffusion models for better accuracy of the extracted electrical characteristics. The device simulation conditions for the electrostatic, analog and RF characteristics of the device are tabulated in Table 2.

Table 2. Device simulation conditions [37]

Electrical Characteristics	V_{ds} (V)	V_{gs} (V)		
		$V_{Initial}$	V_{Step}	V_{Final}
On-state Current, I_{ON} (µA/µm)	0.5	0	0.1	1.0
Off-state Current, I_{OFF} (pA/µm)	0.5	0	0.1	1.0
On–off ratio	0.5	0	0.1	1.0
Transconductance, g_m (mS/µm)	0.5	0	0.1	1.0
Cut-off frequency, f_T (GHz)	0.5	0	0.1	1.0
Maximum oscillation frequency, f_{max} (GHz)	0.5	0	0.1	1.0

Figure 4 shows the initial I_{ds}-V_{gs} transfer characteristics in both linear and log mode, shifting the curve towards maximum V_{gs} of 1V. From the curve, the extracted magnitude of I_{ON}, I_{OFF} and on-off ratio are observed to be 1226.3 µA/µm, 114212 pA/µm and 0.011 x 10^6 respectively. The transconductance (g_m) is an important analog characteristic that measures how minimum the V_{gs} is needed to increase the I_{ds} of a transistor. Generally, the g_m is used to measure the gain, cut off frequency (f_T) and maximum oscillation frequency (f_{max}) of an amplifier, which can be calculated as:

$$g_m = \frac{\partial I_{ds}}{\partial V_{gs}} \tag{1}$$

Apart from g_m, the intrinsic capacitances such as gate-to-source capacitance (C_{gs}) and gate-to-drain capacitance (C_{gd}) are also regarded as the main components to measure the RF

performance of the device. A small signal with a constant frequency (f) of 1 MHz was applied to the gate terminal in order to extract the magnitude of the intrinsic capacitances for measuring the f_T and f_{max} of the device. The intrinsic capacitances (C_{gs} & C_{gd}) as a function of V_{gs} at a constant V_{ds} of 0.5V are shown in Figure 5.

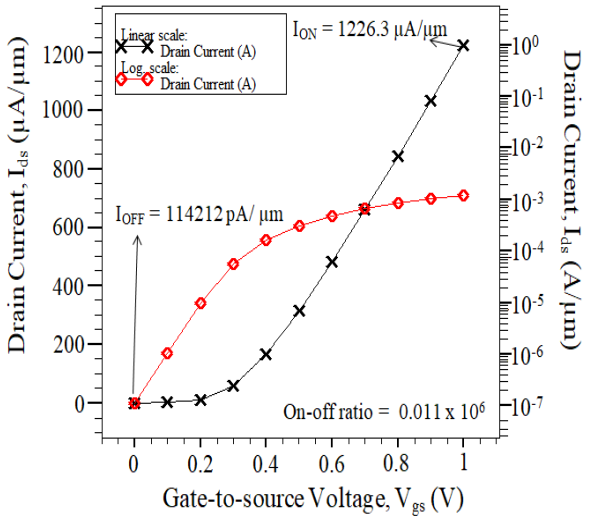

Figure 4. Initial Plot of I_{ds}-V_{gs} transfer characteristics at a constant V_{ds} = 0.5V.

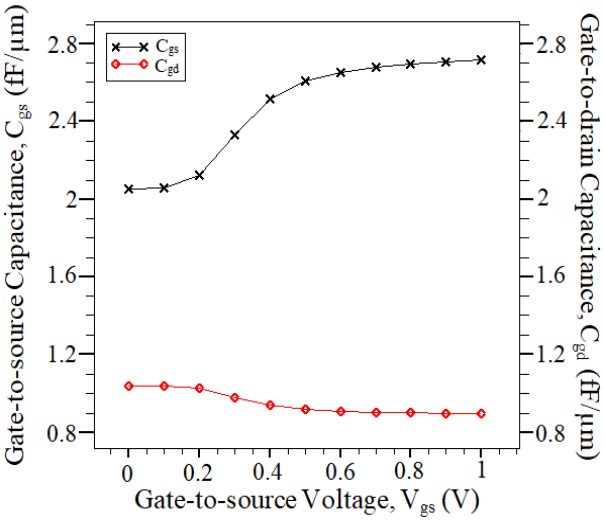

Figure 5. Initial Plot of C_{gs} and C_{gd} as a function of V_{gs} at V_{ds} = 0.5V

It is observed that C_{gs} starts to increase as V_{gs} reach saturation mode. After saturation, the C_{gs} value becomes constant towards maximum V_{gs}. However, the C_{gd} is observed to be almost constant as the gate bias is shifted to its maximum. The C_{gs} and C_{gd} values are desired to be as small as possible in order to attain much higher f_T and f_{max}. The f_T of the device can be calculated by the following equation:

$$f_T = \frac{g_m}{2\pi(C_{gs} + C_{gd})} \quad (2)$$

The magnitude of f_T can be regarded as an excellent indicator for low-current forward transit time. However, it is not suitable for a performance indicator because it neglects the impact of the gate resistance (R_g). Thus, the f_{max} that includes the R_g component is proposed. The f_{max} can be regarded as the maximum frequency that allows the power gain being drawn out from a transistor. The f_{max} for the n-JLDGVM device can be mathematically described as:

$$f_{\max} = \sqrt{\frac{f_T}{8\pi R_g C_{gd}}} \tag{3}$$

where,

$$R_g = \frac{1}{2\pi f_T (C_{gs} + C_{gd})} \tag{4}$$

The initial extracted electrical characteristics of the n-JLDGVM device are summarized in Table 3.

Table 3. Initial electrical characteristics

Electrical Characteristics	Unit	Value
On-state Current, I_{ON}	µA/µm	1226.3
Off-state Current, I_{OFF}	pA/µm	114212
On–off ratio	N/A	0.011×10^6
Transconductance, g_m	mS/µm	1.92
Cut-off frequency, f_T	GHz	84.4
Maximum oscillation frequency, f_{max}	GHz	1935

OPTIMAL DESIGN VIA HYBRID TAGUCHI-GREY RELATIONAL ANALYSIS

Taguchi method is a well-known statistical analysis used in various engineering optimization. It consists of a special orthogonal array (OA) which is used to design systematic experiments. Due to the limitation on multi-objective optimization problems, Taguchi method is then incorporated with the Grey relational analysis (GRA). GRA is originally based on Grey theory, applicable to a system in which the model contains uncertain or incomplete information. Figure 6 shows the optimization process workflow for n-JLDGVM device using hybrid Taguchi-GRA.

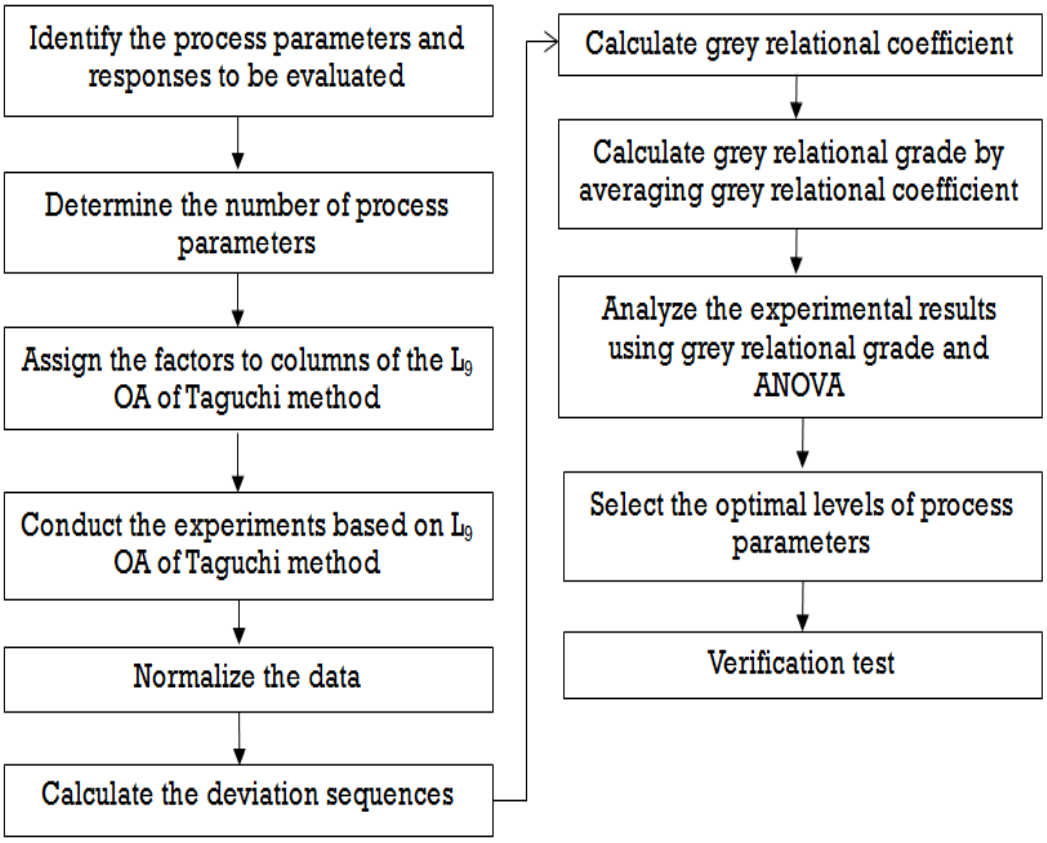

Figure 6. Optimization Process Workflow via Taguchi-GRA

L_9 Orthogonal Array (OA) of Taguchi Method

In this study, four design parameters used in constructing the n-JLDGVM device are optimized simultaneously via hybrid Taguchi-GRA. The investigated design parameters are channel length (L_{ch}), pillar thickness (L_p), channel doping (N_{ch}), S/D doping (N_{sd}) and each of them are varied into three different levels as shown in Table 4.

Table 4. Design parameters of n-JLDGVM device.

Symbols	Design Parameter	Units	Level 1	Level 2	Level 3
A	Channel Length, L_{ch}	nm	9	10	11
B	Pillar Thickness, L_p	nm	8	9	10
C	Channel doping, N_{ch}	Atom/cm^3	1x10^{18}	5x10^{18}	9x10^{18}
D	S/D doping, N_{sd}	Atom/cm^3	1x10^{18}	5x10^{18}	9x10^{18}

Since this design only involved four process parameters, the L_9 OA of Taguchi method is opted for data acquisition. The electrical characteristics with the corresponding design parameter levels are retrieved based on the L_9 OA as tabulated in Table 5. The information in the Table 5 is used to further analyze the impact of the design parameters on multiple electrical characteristics of the device.

Normalization and Deviation Sequences

The magnitude of I_{ON}, I_{OFF}, on-off ratio, g_m, f_T and f_{max} are then normalized based on their corresponding type of problems. For instance, I_{ON}, on-off ratio, g_m, f_T and f_{max} are always desired to be as large as possible, thus the experimental data should be normalized using larger-the-better (LTB) type of problem.

Table 5. Electrical Characteristics based on L_9 OA of Taguchi Method

Exp no.	Parameter Level				I_{ON} (μA/μm)	I_{OFF} (pA/μm)	On-off ratio (x10^6)	g_m (mS/μm)	f_T (GHz)	f_{max} (Ghz)
	A	B	C	D						
1	1	1	1	1	2328.5	2.47	942.7	4.71	120.6	2455
2	1	2	2	2	2500.6	43.2	57.9	4.61	115.8	2270
3	1	3	3	3	2369	242511	0.0098	3.39	73.2	1737
4	2	1	2	3	1117	57923	0.019	1.8	103.6	2305
5	2	2	3	1	1594.5	2735787	0.00058	2.02	89.2	1994
6	2	3	1	2	838.8	2112.2	0.397	1.69	80.3	1818
7	3	1	3	2	1180.5	613.6	1.9	2.39	59.3	1571
8	3	2	1	3	456.1	14.2	32.1	1.74	43	1273
9	3	3	2	1	815.9	12774	0.06	1	53.9	1491

In contrast, the magnitude of I_{OFF} is always desired to be as small as possible, hence its corresponding experimental data should be normalized using smaller-the-better (STB) type of problem. The normalization process for both type of problems can be performed using the following equations:

$$x_i^*(k) = \frac{x_i(k) - \min x_i(k)}{\max x_i(k) - \min x_i(k)}, \text{ LTB} \tag{5}$$

$$x_i^*(k) = \frac{\max x_i(k) - x_i(k)}{\max x_i(k) - \min x_i(k)}, \text{ STB} \tag{6}$$

where xi*(k) and xi(k) are the sequence after data pre-processing and comparability sequence. After the normalization process, the deviation sequences of each experiment rows are then computed. The Δoi (k) represents the deviation sequence of the reference sequence xo* (k) and the comparability sequence xi*(k) and it can be computed by using:

$$\Delta_{oi}(k) = | x_o^*(k) - x_i^*(k) | \tag{7}$$

where the reference sequence xo* (k) is equal to 1. Table 6 tabulates the deviation sequences of all the electrical characteristics that correspond to their type of problems.

Grey Relational Coefficient and Grade

From the computed deviation sequences in Table 4, a Grey relational coefficient (GRC) is then calculated by using:

$$\xi(k) = \frac{\Delta_{\min} + \xi\Delta_{\max}}{\Delta_{oi}(k) + \xi\Delta_{\max}} \tag{8}$$

where ξ is a n identification coefficient, Δ_{max} is a maximum absolute difference and Δ_{min} is a minimum absolute difference. The value of ξ is fixed to 0.5 due to the fact that all the design parameters are given an equal preference.

Table 6. Deviation Sequences Based on L_9 OA of Taguchi-GRA

Exp. no	Deviation Sequence, $\Delta_{oi}(k)$					
	Δ_{oi} (I_{ON})	Δ_{oi} (I_{OFF})	Δ_{oi} (On-off ratio)	Δ_{oi} (g_m)	Δ_{oi} (f_T)	Δ_{oi} (f_{max})
1	0.084177	0	0		0	0
2	0	1.49E-05	0.938581	0.026954	0.061856	0.156514
3	0.064368	0.088643	0.99999	0.355795	0.610825	0.607445
4	0.676742	0.021171	0.99998	0.784367	0.219072	0.126904
5	0.443189	1	1	0.725067	0.404639	0.390017
6	0.812815	0.000771	0.999579	0.814016	0.51933	0.538917
7	0.645684	0.000223	0.997985	0.625337	0.789948	0.747885
8	1	4.29E-06	0.965949	0.800539	1	1
9	0.824016	0.004668	0.999937	1	0.859536	0.815567

Based on the computed GRC, the Grey relational grades (GRG) are simply measured by taking the average of all the GRC of the electrical characteristics. The rank of each experiment is determined based on the highest calculated GRG. The experiment rows with higher GRG imply that the corresponding level of the design parameters have a better quality of multi-response characteristics. Table 7 shows the calculated GRC, GRG and their ranks for each of the experiment rows.

Table 7. Grey relational coefficients based on L_9 OA of Taguchi-GRA

Exp. no.	GRC						GRG (γ_i)	Rank
	ξ_i (I_{ON})	ξ_i (I_{OFF})	ξ_i (on-off ratio)	ξ_i (g_m)	ξ_i (f_T)	ξ_i (f_{max})		
1	0.855905	1	1	1.053908	1	1	0.984969	1
2	1	0.99997	0.347565	1	0.889908	0.761598	0.833174	2
3	0.885947	0.849411	0.333336	0.615748	0.450116	0.45149	0.597675	4
4	0.424902	0.959377	0.333338	0.410283	0.695341	0.797571	0.603469	3
5	0.530116	0.333333	0.333333	0.430143	0.552707	0.561787	0.456903	9
6	0.380861	0.99846	0.333427	0.401026	0.490518	0.48127	0.51426	5
7	0.436421	0.999553	0.333782	0.468263	0.387612	0.400678	0.504385	6
8	0.333333	0.999991	0.341076	0.405181	0.333333	0.333333	0.457708	8
9	0.377639	0.99075	0.333347	0.351303	0.367773	0.380064	0.466813	7

GRG for the Level of Design Parameters

According to Table 6, the experiment row no. 1 exhibits the highest GRG, implying it has the best multi-response characteristics among other rows. The GRGs at multiple levels can be separated out since the DoE of L_9 Taguchi method is orthogonally distributed. For instance, the average of GRG for level 1 of the parameter A (channel length) is calculated

based on the allocation of level 1 in the parameter A's column as shown in Table 5. In this case, the GRG (γi) for level 1 of design parameter A (channel length) can be measured using:

$$\gamma_{A1} = \frac{1}{3}[\gamma_1 + \gamma_2 + \gamma_3] \quad (9)$$

The similar step was repeated for the remaining design parameters. All the calculated GRG for each level of design parameters are tabulated in Table 8. The GRGs for each design parameters are then transformed into parameter effect plots for better data interpretation as depicted in Figure 7.

Table 8. Average GRG by level of design parameters

Symbols	Design Parameters	Grey Relational Grade		
		Level 1	Level 2	Level 3
A	Channel Length, L_{ch}	0.80527	0.52488	0.47630
B	Pillar Thickness, L_p	0.69761	0.58259	0.52624
C	Channel doping, N_{ch}	0.65231	0.63448	0.51965
D	S/D doping, N_{sd}	0.63623	0.61727	0.55295

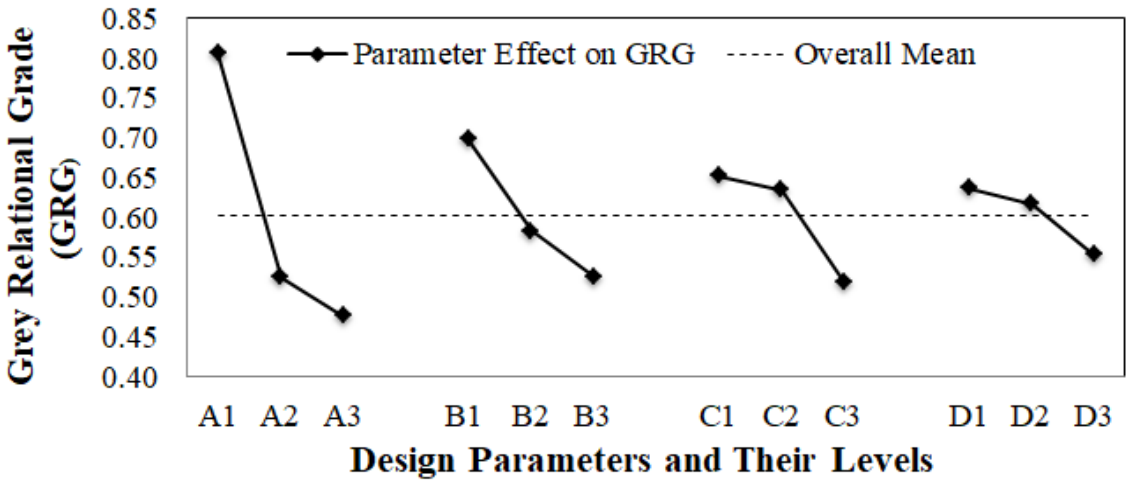

Figure 7. Parameter effect plot of GRG for multi-response characteristics.

The level of design parameters that demonstrated the highest GRG was regarded as the optimal parameter level for n-JLDGVM device. Based on the plots, it is observed that the most optimum levels of the design parameters are $A_1B_1C_1D_1$.

Analysis of Variance (ANOVA) for GRG

The significance of each design parameters towards the GRG can be determined via analysis of variance (ANOVA). In this study, ANOVA was utilized to separate the total variability of the GRGs measured by the sum of the squared deviations from the overall mean of GRGs. The sum of squares (SS) of each design parameter and error were then transformed into percentage contribution which provided the level of significance for each design parameter towards the GRG. In general, the ANOVA table comprises specific parameters such as sum

of squares (SSQ), degree of freedom (DF), variance or mean square (MS), F-value and contribution of a parameter. The total sum of the squared deviation (SS_T) from the overall mean GRG (γ_m) can be measured by using:

$$SS_T = \sum_{j=1}^{p} \left(\gamma_j - \gamma_m\right)^2 \tag{10}$$

where p is the number of the experiments in the OA and γ_j is the mean of the GRG for j^{th} experiment. The SS_T can be disintegrated into the sum of the squared deviations of a design parameter (SS_q) and the sum of the squared deviations of errors (SS_e). The SS_q of a design parameter can be calculated using:

$$SS_{q(X)} = k\left[\sum_{j=1}^{k} (\gamma_{Xj} - \gamma_m)^2\right] \tag{11}$$

where X represents a design parameter, k is the number of levels for the GRG, j is the level of GRG and γ_{Xj} is the GRG of a certain level of the design parameter. Meanwhile, the SS_e can be calculated using:

$$SS_e = \frac{SS_T}{m(k-1)} \tag{12}$$

where SS_T is the total sum of the squared deviation, m is the number of factors and k is the number of levels for the GRG. The mean squares of a factor (MS_q) and an error (MS_e) were then calculated by dividing their sum of squares with their corresponding degree of freedom (DF) as follows:

$$MS_{q(X)} = \frac{SS_{q(X)}}{DF} \tag{13}$$

$$MS_e = \frac{SS_e}{DF} \tag{14}$$

where $SS_{q(X)}$ is the sum of squared for a design parameter and DF is the degree of freedom for a design parameter. Subsequently, the F-test was performed to recognize which design parameters contributed a significant impact on GRG. The large value of F normally implied that the variation in a certain design parameter had a major effect on the GRG. The F-value for a design parameter can be estimated as:

$$F_{q(X)} = \frac{MS_{q(X)}}{MS_e} \tag{15}$$

where $MS_{q(X)}$ is the mean squares of a certain factor and MS_e is the mean squares of error. The percentage contribution (ρ) for a design parameter can be calculated using:

$$P_{q(X)} = \frac{SS_{q(X)}}{SS_{qT}} \tag{16}$$

where $SS_{q(X)}$ is the sum of squares for a design parameter and $SS_{q(T)}$ is the total sum of square for all the design parameter including the error. The completed results of ANOVA and the percentage contribution of the design parameters on GRG are shown in Table 9 and Figure 8 respectively. According to Figure 8, the most significant design parameter is channel length (L_{ch}) with approximately 50.1% parameter effect on GRG, followed by followed by pillar thickness with 24.3% parameter effect on GRG and channel doping with 16.5% factor effect on GRG. The least significant design parameter is found to be S/D doping with approximately

6.1% parameter effect on GRG. Thus, S/D doping can be regarded as an adjustment parameter to tune the overall n-JLDGVM's performance since it has the least impact on GRG.

Table 9. Results of ANOVA for GRG

Symbol	Design Parameter	DF	SSQ	MS	F-ratio	Percentage contribution, ρ (%)
A	Channel Length, L_{ch}	2	0.094459	0.04723	24.80878	50.11874
B	Pillar Thickness, L_p	2	0.045766	0.022883	12.02009	24.28301
C	Channel Doping, N_{ch}	2	0.031102	0.015551	8.168659	16.50234
D	S/D Doping, N_{sd}	2	0.011432	0.005716	3.002474	6.065605
-	Error	3	0.005711	0.001904	-	3.030303
	Total	11	0.188471	0.093284	-	100

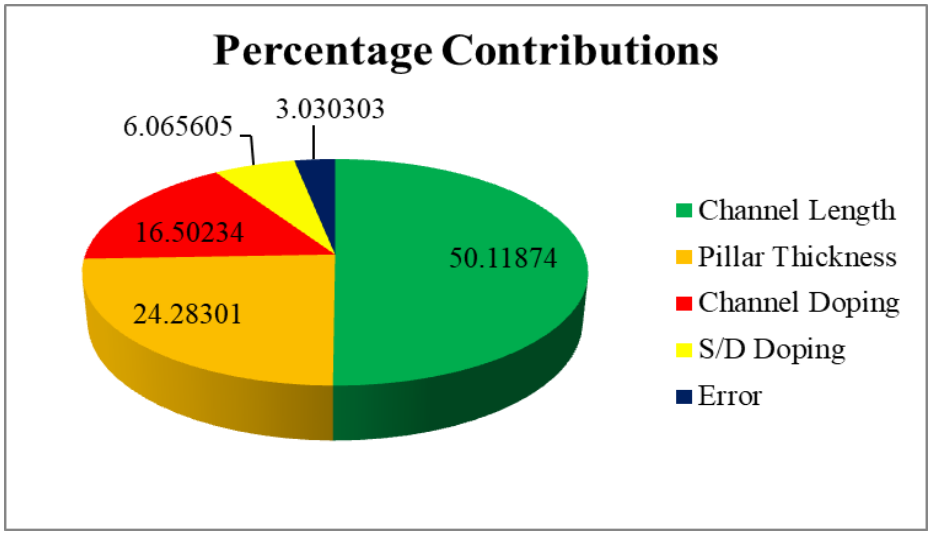

Figure 8. Percentage contributions of design parameters on the GRG.

Verification Test

Confirmation test is performed to confirm the optimum level of the design parameters predicted by L_9 OA of Taguchi-GRA with the actual simulation results. The optimum parameter levels that yield the largest GRG are A1B1C1D1. Table 10 shows the optimum design parameters predicted via L_9 OA of Taguchi-GRA for n-JLDGVM device.

Table 10. Optimum level of design parameters via Taguchi-GRA.

Symbol	Design Parameter	Units	Optimum Value
A	Channel Length, L_{ch}	nm	9
B	Pillar Thickness, L_p	nm	8
C	Channel doping, N_{ch}	Atom/cm^3	1x10^{18}
D	S/D doping, N_{sd}	Atom/cm^3	1x10^{18}

The n-JLDGVM device was re-simulated using the predicted design parameters in Table 10. Apart from that, the GRG of the optimum design parameters can be calculated using:

$$\hat{\gamma} = \gamma_m + \sum_{i=1}^{4} (\gamma_i - \gamma_m) \quad (17)$$

The improvements in GRG with optimized design parameters for multi-response characteristics are summarized in Table 11.

Table 11. Improvements in GRG and multiple electrical characteristics with optimum design parameters.

Condition Description	Before Optimization	After Optimization using L_9 OA of Taguchi-GRA
Level	$A_2B_2C_2D_2$	$A_1B_1C_1D_1$
GRG	0.636785	0.984969
On-state Current, I_{ON} (µA/µm)	1226.3	2328.5
Off-state Current, I_{OFF} (pA/µm)	114212	2.47
On –off ratio	0.011 x 10^6	940 x 10^6
Transconductance, g_m (mS/µm)	1.92	4.71
Cut-off frequency, f_T (GHz)	84.4	120.6
Maximum oscillation frequency, f_{max} (GHz)	1935	2455

From Table 11, the GRG of the design parameters after optimization was improved by approximately 35% compared to the GRG before optimization. The largest GRG after the optimization implied that the predicted design parameters were the best combination for achieving significant improvements on I_{ON}, I_{OFF}, on-off ratio, g_m, f_T and f_{max} of the n-JLDGVM device. The results show that the I_{ON}, on-off ratio, g_m, f_T and f_{max} are improved by 47%, 99.9%, 59%, 30% and 21% respectively. Moreover, the I_{OFF} of n-JLDGVM device after optimization is approximately 451098 times smaller than the I_{OFF} before optimization. Thus, the hybrid L_9 OA of Taguchi-GRA can be regarded as an efficient optimization approach for solving multiple electrical characteristics of the n-JLDGVM device.

OPTIMAL DESIGN VIA EXTENDED ANALYSIS WITH ARTIFICIAL NEURAL NETWORKS PREDICTION

This section describes an extended analysis to further optimize the design parameters towards I_{ON}, I_{OFF}, on-off ratio, g_m, f_T and f_{max} of the n-JLDGVM device with the aid of artificial neural networks (ANN) prediction. In previous section, S/D doping (N_{sd}) has been identified as the least significant parameter on the GRG. Any changes in S/D doping would not contribute much effect on the GRG. Hence, S/D doping is selected as an adjustment parameter to tune the GRG for better electrical characteristics of the device. This extended analysis consists of two stages which are the GRG computation for 18 trials and the ANN training based on Levenberg-Marquardt back propagation (LMBP) algorithm. Figure 9 depicts the process workflow for the extended analysis.

18 Sets of Experiment for GRG Computation

The extended analysis initiates with the design of 18 sets of experiment in which the adjustment parameter (S/D doping) is varied into 18 different values. The other design parameters are fixed to their optimum value as predicted by the previous Taguchi-GRA approach. The electrical characteristics with the corresponding design parameter levels are obtained based on the 18 experiment rows as shown in Table 12. The retrieved data in Table 12 is then employed to compute the GRC for each of experiment row. From Table 12, the electrical characteristics of n-JLDGVM device are normalized based on their corresponding types of problem by using (4) and (5). The normalized data are then pre-processed by measuring the deviation sequences, $\Delta_{oi}\,(k)$ using (6). Table 13 summarizes the computed deviation sequences of all the electrical characteristics in accordance to their type of problems.

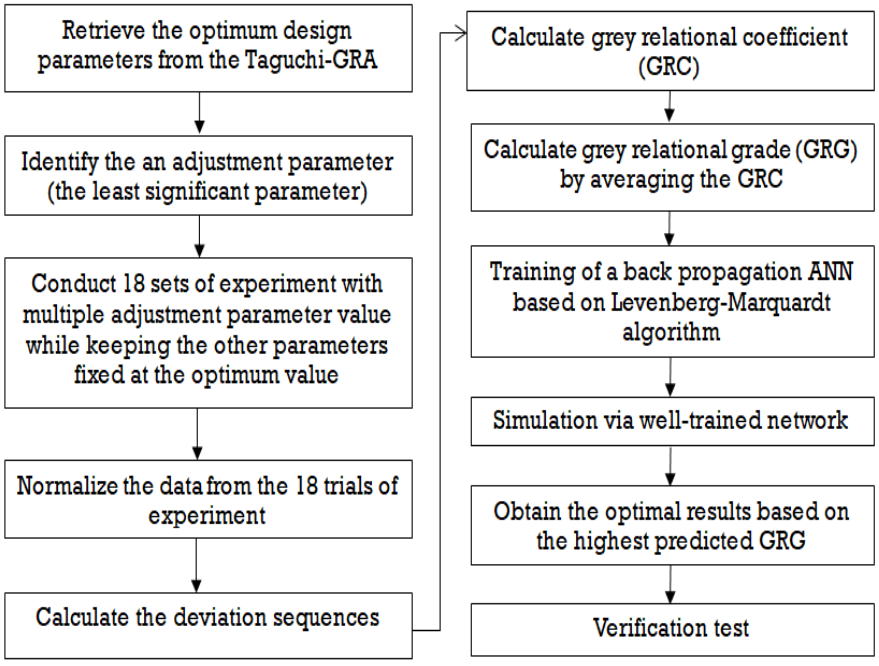

Figure 9. Optimization Process Workflow via extended analysis with a well-trained ANN prediction.

Table 12. Electrical characteristics based on 18 sets of experiment with multiple S/D doping levels

Exp no.	Parameter value				I_{ON} (μA/μm)	I_{OFF} (pA/μm)	On-off ratio ($x10^6$)	g_m (mS/μm)	f_T (GHz)	f_{max} (Ghz)
	L_{ch} (nm)	T_p (nm)	N_{ch} (atom/cm^3)	N_{sd} (atom/cm^3)						
1	9	8	$1x10^{18}$	$1x10^{18}$	2328.5	2.47	942.7	4.714	120.61	2454.99
2	9	8	$1x10^{18}$	$1.4x10^{18}$	2331	2.478	940.7	4.721	120.72	2456.69
3	9	8	$1x10^{18}$	$1.6x10^{18}$	2332.6	2.483	939.3	4.725	120.75	2457.44
4	9	8	$1x10^{18}$	$1.8x10^{18}$	2334.3	2.489	938.3	4.73	120.84	2458.71
5	9	8	$1x10^{18}$	$2x10^{18}$	2335.7	2.491	937.7	4.736	120.92	2459.91
6	9	8	$1x10^{18}$	$2.2x10^{18}$	2336.9	2.494	936.8	4.739	120.96	2460.6
7	9	8	$1x10^{18}$	$2.4x10^{18}$	2337.7	2.497	936.3	4.742	120.99	2461.25
8	9	8	$1x10^{18}$	$2.6x10^{18}$	2338.6	2.499	935.9	4.745	121.05	2462.07
9	9	8	$1x10^{18}$	$2.8x10^{18}$	2339.2	2.5	935.6	4.747	121.07	2462.5
10	9	8	$1x10^{18}$	$3x10^{18}$	2340.2	2.501	935.5	4.753	121.2	2464.06
11	9	8	$1x10^{18}$	$3.2x10^{18}$	2340.3	2.503	935.2	4.751	121.11	2463.29
12	9	8	$1x10^{18}$	$3.4x10^{18}$	2340.8	2.502	935.6	4.753	121.15	2463.88
13	9	8	$1x10^{18}$	$3.6x10^{18}$	2341.2	2.502	935.8	4.755	121.18	2464.29
14	9	8	$1x10^{18}$	$3.8x10^{18}$	2341.6	2.497	937.8	4.756	121.2	2464.61
15	9	8	$1x10^{18}$	$4x10^{18}$	2341.9	2.491	940.3	4.759	121.21	2464.91
16	9	8	$1x10^{18}$	$4.2x10^{18}$	2342.2	2.487	941.9	4.759	121.23	2465.24
17	9	8	$1x10^{18}$	$4.4x10^{18}$	2342.5	2.486	942.3	4.761	121.25	2465.51
18	9	8	$1x10^{18}$	$4.6x10^{18}$	2342.7	2.489	941.3	4.762	121.27	2465.77

The computed deviation sequences are analyzed by identifying the maximum and minimum absolute difference, denoted as Δ_{max} and Δ_{min} respectively. Based on the information, the GRC can be then calculated by using (7). Finally, the GRG for each experiment row is measured by averaging the GRC of all the electrical characteristics. Table 14 lists all the calculated GRC, GRG and their ranks for each of the experiment rows. The experiment rows with higher GRG imply that the respective combinational levels of the design parameters would exhibit a better quality of multi-response characteristics.

Table 13. Deviation sequences based on 18 sets of experiment.

Exp. No	Deviation Sequence, $\Delta_{oi}(k)$					
	$\Delta_{oi}(I_{ON})$	$\Delta_{oi}(I_{OFF})$	Δ_{oi} (On-off ratio)	$\Delta_{oi}(g_m)$	$\Delta_{oi}(f_T)$	$\Delta_{oi}(f_{max})$
1	1	0	0	1	1	1
2	0.823944	0.242424	0.266667	0.854167	0.833333	0.842301
3	0.711268	0.393939	0.453333	0.770833	0.787879	0.772727
4	0.591549	0.575758	0.586667	0.666667	0.651515	0.654917
5	0.492958	0.636364	0.666667	0.541667	0.530303	0.543599
6	0.408451	0.727273	0.786667	0.479167	0.469697	0.479592
7	0.352113	0.818182	0.853333	0.416667	0.424242	0.419295
8	0.288732	0.878788	0.906667	0.354167	0.333333	0.343228
9	0.246479	0.909091	0.946667	0.3125	0.30303	0.30334
10	0.176056	0.939394	0.96	0.1875	0.106061	0.158627
11	0.169014	1	1	0.229167	0.242424	0.230056
12	0.133803	0.969697	0.946667	0.1875	0.181818	0.175325
13	0.105634	0.969697	0.92	0.145833	0.136364	0.137291
14	0.077465	0.818182	0.653333	0.125	0.106061	0.107607
15	0.056338	0.636364	0.32	0.0625	0.090909	0.079777
16	0.035211	0.515152	0.106667	0.0625	0.060606	0.049165
17	0.014085	0.484848	0.053333	0.020833	0.030303	0.024119
18	0	0.575758	0.186667	0	0	0

Table 14. Grey relational coefficients and grades based on 18 sets of experiment.

Exp. no.	GRC						GRG (γ_i)	Rank
	$\xi_i(I_{ON})$	$\xi_i(I_{OFF})$	ξ_i (on-off ratio)	$\xi_i(g_m)$	$\xi_i(f_T)$	$\xi_i(f_{max})$		
1	0.333333	1	1	0.333333	0.333333	0.333333	0.555556	10
2	0.37766	0.673469	0.652174	0.369231	0.375	0.372495	0.470005	15
3	0.412791	0.559322	0.524476	0.393443	0.388235	0.392857	0.445187	18
4	0.458065	0.464789	0.460123	0.428571	0.434211	0.432932	0.446448	17
5	0.503546	0.44	0.428571	0.48	0.485294	0.479111	0.46942	16
6	0.550388	0.407407	0.388601	0.510638	0.515625	0.510417	0.480513	14
7	0.586777	0.37931	0.369458	0.545455	0.540984	0.543895	0.494313	13
8	0.633929	0.362637	0.35545	0.585366	0.6	0.592959	0.521724	12
9	0.669811	0.354839	0.345622	0.615385	0.622642	0.622402	0.53845	11
10	0.739583	0.347368	0.342466	0.727273	0.825	0.759155	0.623474	7
11	0.747368	0.333333	0.333333	0.685714	0.673469	0.684879	0.57635	9
12	0.788889	0.340206	0.345622	0.727273	0.733333	0.740385	0.612618	8
13	0.825581	0.340206	0.352113	0.774194	0.785714	0.784571	0.64373	6
14	0.865854	0.37931	0.433526	0.8	0.825	0.822901	0.687765	5
15	0.898734	0.44	0.609756	0.888889	0.846154	0.8624	0.757656	4
16	0.934211	0.492537	0.824176	0.888889	0.891892	0.910473	0.823696	3
17	0.972603	0.507692	0.903614	0.96	0.942857	0.953982	0.873458	1
18	1	0.464789	0.728155	1	1	1	0.865491	2

A Well-Trained ANN Prediction

Artificial neural networks (ANN) are defined as computational systems specifically designed to emulate a simulation for neurons of biological nervous systems. The ANN in this study is based on Levenberg-Marquardt back propagation (LMBP) algorithm. The LMBP is preferred due to its faster training time. A network topology of the ANN based on LMBP consists of one neuron for S/D doping parameter in input layer, 10 neurons for single hidden layer and one neuron for single output layer which expressing a relationship between input and output layers as clearly shown in Figure 10. The network performance is evaluated via training and testing of a set of data. The quality of prediction is determined by computing the mean squared error (MSE) of the predicted values from the actual measured data. MSE provides. The tested data set with smaller MSE implies the better quality of the prediction. The MSE can be mathematically expressed by:

$$MSE = \frac{1}{n}\sum_{t=1}^{n}(P_t - A_t)^2 \tag{18}$$

where F_t is the predicted value and A_t is the actual value. The neuron model for the hidden layer of the LMBP network is based on hyperbolic tangent sigmoid transfer function "Tansig", while the neuron model for the output layer is based on linear transfer function "Pureln". Therefore, the network outputs can take on any value and not limited between 0 and 1 as the neuron's net input goes from negative to positive infinity. The best quality of multiple electrical characteristics of the n-JLDGVM device is determined based on the highest predicted GRG. The division of the experimental data are set up in which four input vectors and a target vector are randomly allocated with 70% used for training, 15% for validation and 15% for testing. For small data sets, it is recommended to use 70:15:15 ratio for 10 fold cross-validation method in order to prevent overfitting. The 10 fold cross-validation method is preferred over the leave-one-out cross validation method because it only requires less number of training. Leave-one-out would produce better results in small data sets but time consuming. For instance, the training using 10 fold cross-validation method with 70:15:15 ratio only requires seven iterations at 0.00 seconds. The linear regression between the network output and the corresponding target for 18 sets of experimental data is depicted in Figure 11.

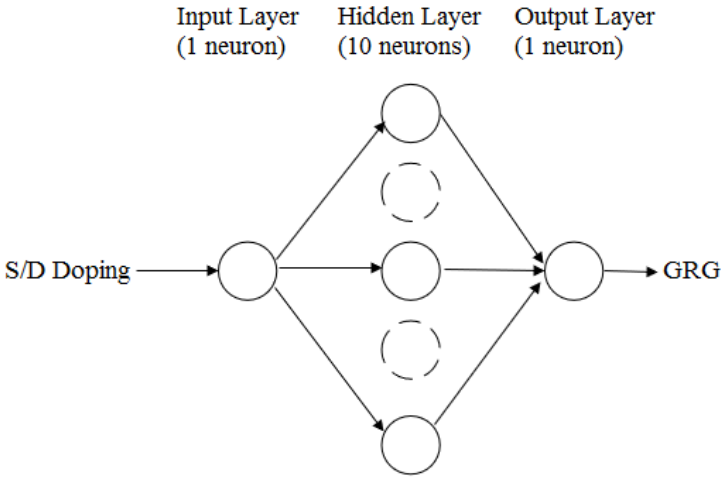

Figure 10. The LMBP Network Topology.

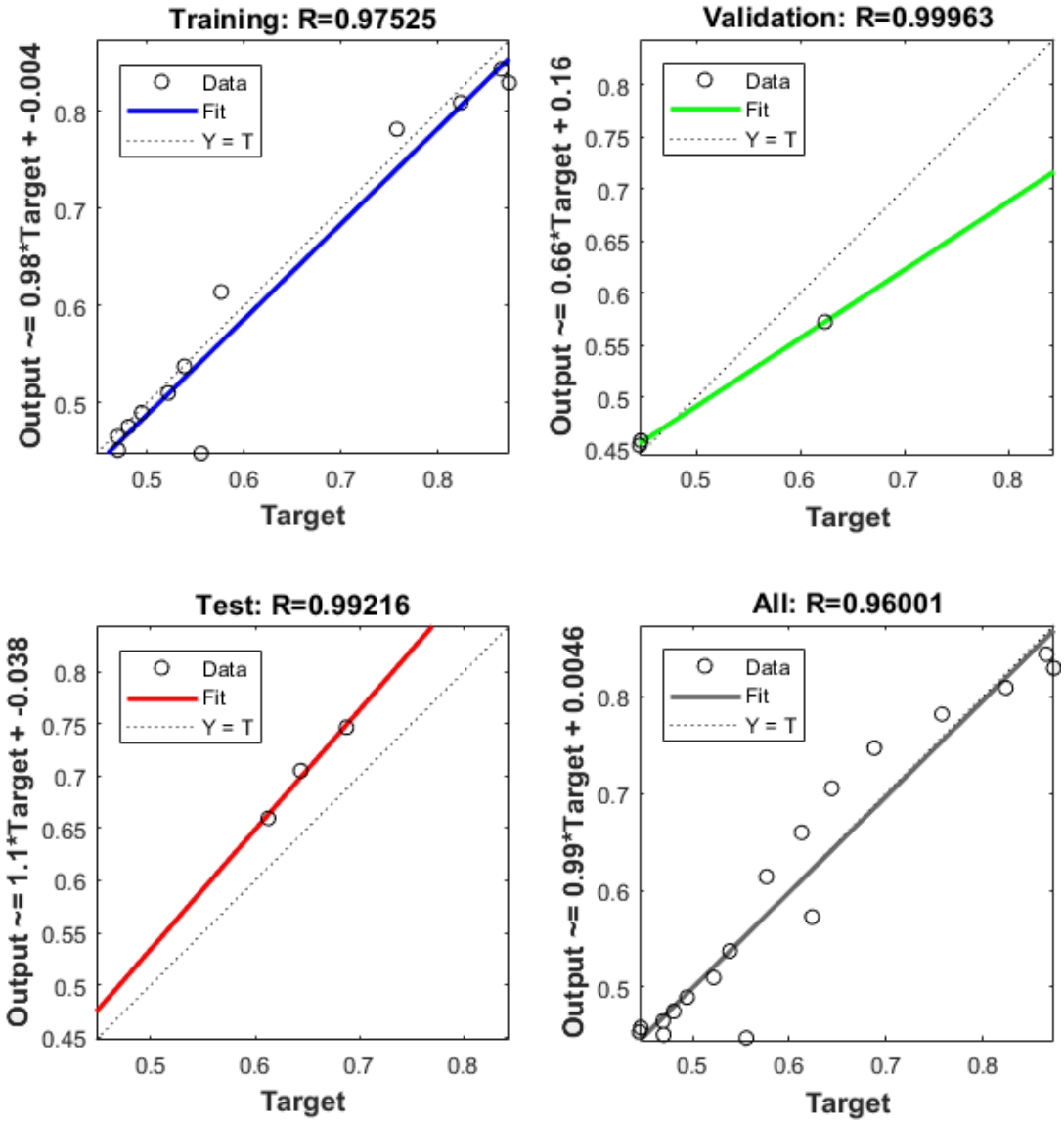

Figure 11. The Regression Plot for LMBP Algorithm

Table 15 shows the prediction outputs of the 18 sets of experiments based on LMBP algorithm. The predictive capability of the developed ANN is evaluated by computing the % net error in the prediction of GRG for 18 experimental rows. The maximum and minimum net error for the 18 sets of experimental data are 10.8% and 0.11%, observed at row 1 and 9 respectively.

Table 15. Predicted GRGs via well-trained ANN.

Exp. No.	Actual GRG	Predicted GRG via ANN	Net Error	Net Error (%)
1	0.555556	0.447571066	0.10798449	10.8
2	0.470005	0.450804852	0.019199892	1.92
3	0.445187	0.453782798	0.008595579	0.86
4	0.446448	0.458290435	0.011842163	1.18
5	0.46942	0.465050056	0.004370404	0.44
6	0.480513	0.475046003	0.005466664	0.55
7	0.494313	0.489526265	0.004786825	0.48
8	0.521724	0.50988844	0.011835113	1.18
9	0.53845	0.537356807	0.001093213	0.11
10	0.623474	0.572406107	0.051068087	5.11
11	0.57635	0.614085874	0.037736199	3.77
12	0.612618	0.659691314	0.047073335	4.71
13	0.64373	0.705263338	0.061533556	6.15
14	0.687765	0.746854196	0.059089066	5.91
15	0.757656	0.781785669	0.024130168	2.41
16	0.823696	0.809134244	0.014561993	1.46
17	0.873458	0.829392068	0.04406609	4.41
18	0.865491	0.843790076	0.021700602	2.17

After the network has been trained, tested and validated, the GRG for the S/D doping with the concentration range from 4.8 x10^{18} atom/cm^3 to 9.8 x10^{18} atom/cm^3 are then predicted. The outcomes of the GRG prediction are plotted in Figure 12.

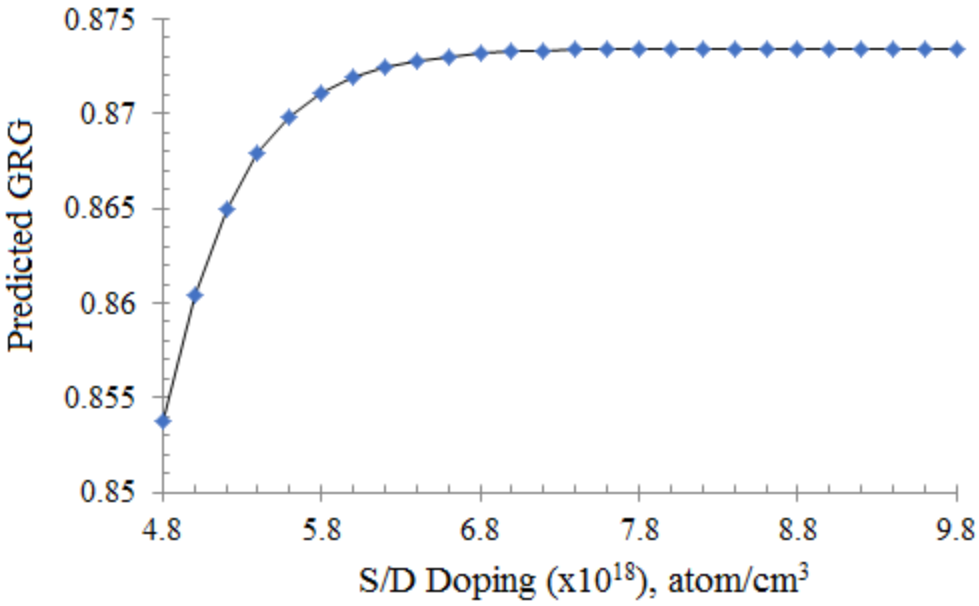

Figure 12. Predicted GRG for Multiple Level of S/D Doping via ANN

Based on the results, the S/D doping is increasing linearly with the predicted GRG at the beginning. After reaching 9.8 x10^{18} atom/cm^3 of doping concentration, the value of predicted GRG begins to saturate as higher doping concentration being applied. The optimal device with S/D doping of 9.8 x10^{18} atom/cm^3 exhibits the largest predicted GRG which is measured at 0.8734. In this case, GRG is utilized as a single unit representing the six electrical characteristics (I_{ON}, I_{OFF}, on-off ratio, g_m, f_T and f_{max}) of the device. Thus, it can be concluded that the most optimum value for channel length (L_{ch}), pillar thickness (T_p), channel doping (N_{ch}) and source/drain doping (N_{sd}) are 9nm, 8nm, 1x10^{18} atom/cm^3 and 9.8 x10^{18} atom/cm^3 respectively. In the next sub-section, these design parameter values predicted by a well-trained ANN will be re-simulated for verification.

Verification Test

Verification test is carried out to justify the optimum design parameters predicted by the ANN prediction with the actual simulated results. Table 16 summarizes the simulation results before optimization, after optimization via L_9 OA of Taguchi-GRA and after optimization via L_9 OA of Taguchi-GRA with ANN prediction. It is observed that the device optimized using Taguchi-GRA with ANN demonstrates an approximate 48% increase in I_{ON} magnitude. Although, the device optimized via L_9 OA of Taguchi-GRA with ANN prediction demonstrates a marginal decrease in on-off ratio for approximately 1.4% compared to the analysis without ANN prediction, it still exhibits a slightly 1.5% increase in g_m magnitude which is considerably good for operational transconductance amplifiers. Apart from g_m, the f_T of the n-JLDGVM device is also increased by approximately 31% via Taguchi-GRA with ANN prediction. The magnitude of f_T significantly relies on the magnitude of g_m since the variation of intrinsic capacitances is almost indistinct. Smaller value of parasitic capacitances is significantly required to gain much higher f_T for high frequency RF applications. Similar trend is also observed in f_{max} in which its magnitude is increased by approximately 22% after being optimized using Taguchi-GRA with ANN prediction.

Table 16. Overall optimization results for n-JLDGVM device.

Design Parameters & Electrical Characteristics	Unit	Before optimization	After optimization via L_9 OA of Taguchi-GRA	After optimization via L_9 OA of Taguchi-GRA with ANN prediction
Channel Length, L_{ch}	nm	10	9	9
Pillar Thickness, L_p	nm	9	8	8
Channel Doping, N_{ch}	Atom/cm^3	5x10^{18}	1x10^{18}	1x10^{18}
S/D Doping, N_{sd}	Atom/cm^3	5x10^{18}	1x10^{18}	9.8x10^{18}
On-state Current, I_{ON}	µA/µm	1226.3	2328.5	2344.9
Off-state Current, I_{OFF}	pA/µm	114212	2.47	2.53
On –off ratio	-	0.011 x 10^6	940 x 10^6	927 x 10^6
Transconductance, g_m	mS/µm	1.92	4.71	4.78
Cut-off frequency, f_t	GHz	84.4	120.6	121.5
Maximum oscillation frequency, f_{max}	GHz	1935	2455	2469

There is a marginal improvement on the several performances of the device after the predictive analysis via ANN in which the magnitude of I_{ON}, g_m, f_t and f_{max} are slightly increased by ~0.7%, ~1.5%, ~0.7% and ~0.6% respectively compared to optimization without ANN prediction. However, the on-off ratio of the device experiences a marginal decline by approximately 1.3% compared to optimization without ANN prediction. This is predominantly due to the fact that the magnitude of I_{OFF} always becomes larger as the I_{ON} is increased. Therefore, the main function of GRA is to assist the optimization process in finding the best level of design parameters for more tolerable and balanced electrical characteristics. With the aid of ANN, the more robust solutions could be predicted even at the outside of specified upper and lower boundaries. Hence, it can be concluded that the L_9 OA of Taguchi-GRA with ANN prediction is one of the effective approaches to simultaneously optimize multiple design parameters for better and more tolerable n-JLDGVM device performances.

CONCLUSIONS

In summary, a proposed optimization approach which incorporates Taguchi method, Grey relational analysis (GRA) and artificial neural networks (ANN) prediction has been employed for optimal design of n-type junctionless vertical double-gate MOSFET (n-JLDGVM). The optimization process involves four design parameters which are channel length (L_{ch}), pillar thickness (T_p), channel doping (N_{ch}) and source/drain doping (N_{sd}). The primary objective of the optimization is to predict the most optimum design parameters for the feasible magnitude of I_{ON}, I_{OFF}, on-off ratio, g_m, f_t and f_{max} for n- JLDGVM device. The key idea of this proposed approach is to merge multiple electrical characteristics into a single unit called Grey relational grade (GRG). The L_9 OA of Taguchi method is then utilized to predict the largest GRG and the adjustment parameter. The optimization process is further enhanced by tuning the adjustment parameter (N_{sd}) with the aid of ANN prediction based on Levenberg-Marquardt back propagation (LMBP) algorithm. Finally, the most optimum design parameters and electrical characteristics of the device have been successfully revealed based on the largest predicted GRG which is 0.8734. Thus, it can be concluded that the L_9 OA of Taguchi-GRA with ANN prediction is an effective approach to simultaneously optimize multiple design parameters and electrical characteristics for n-JLDGVM device.

ACKNOWLEDGEMENTS

The authors would like to thank to the Universiti Teknikal Malaysia Melaka for laboratory facilities and financial assistance under Fundamental Research Grant project no: FRGS/1/2017/TK04/FKEKK-CeTRI/F00335.

REFERENCES

[1] Ramakrishnan H. Variability: Analysis and Impact on Circuit Response. 2009.

[2] ITRS. International Technology Roadmap Semiconductor. 2013.

[3] Frank DJ, Dennard RH, Nowak E, Solomon PM, Taur Y, and Wong HP. Device Scaling Limits of Si MOSFETs and Their Application Dependencies. Proceeding of IEEE. 2001;89(3):259–288.

[4] Bedell SW, Majumdar A. Ott JA, Arnold J, Fogel K, Koester SJ and Sadana DK. Mobility scaling in short-channel length strained Ge-on-insulator P-MOSFETs. IEEE Electron Device Letter. 2008;29(7):811–813.

[5] Pradhan KP, Mohapatra SK, and Sahu PK. Impact of Channel and Metal GateWork Function on GS-DG MOSFET: A Linearity Analysis. ECS Journal of Solid State Science and Technology. 2015;4(9):1–5.

[6] Zain ASM. Scaling and Variability in Ultra Thin Body Silicon on Insulator (UTB SOI) MOSFETs. University of Glasgow. 2013.

[7] Rezali FA, Mazhar M, Aida N, Othman F, and Muhamad SW. Performance and device design based on geometry and process considerations for 14 / 16 - nm FinFETs stress engineering. IEEE Transactions on Electron Devices. 2016;63(3):974–981.

[8] Hoeneisen B and Mad CA. Fundamental Limitation in Microelectronics –I.MOS Technology. Solid-State Electronics. 1972;15:819–829.

[9] Hagiwara T, Yamaguchi K and Asai S. Threshold voltage variation in very small MOS transistors due to local dopant fluctuations. Proceeding **S**ymposium on VLSI Technology Digest of Technical Papers. 1982;46–47.

[10] Asenov A. Statistically reliable 'Atomistic' simulation of Sub 100nm MOSFETs. Simulation of Semiconductor Process and Devices. 1998;223–226.

[11] Asenov A, Brown AR, Davies JH, Kaya S and Slavcheva G. Simulation of intrinsic parameter fluctuations in decananometer and nanometer-scale MOSFETs. IEEE Transactions on Devices. 2003;50(9):1837–1852.

[12] Asenov A, Kaya S and Davies JH. Intrinsic Threshold Voltage fluctuations in Decanano MOSFETs Due to Local Oxide Thickness Variations. IEEE Transactions on Devices. 2002;49(1):112–119.

[13] Asenov A, Kaya S and Brown AR. Intrinsic Parameter Fluctuations in Decananometer MOSFETs Introduced by Gate Line Edge Roughness. IEEE Transactions on Devices. 2003;50(5):1254–1260.

[14] Yussoff AR, Suffian MRZM and Taib MY. Literature Review of Optimization Techniques for Chatter Suppression in Machining. Journal of Mechanical Engineering and Sciences. 2011;1:47–61.

[15] Salehuddin F, Kaharudin KE, Zain ASM, Yamin AKM, and Ahmad I. Analysis of process parameter effect on DIBL in n-channel MOSFET device using L_{27} orthogonal array. International Conferences on Fundamental and Applied Sciences. 2014;1621(1):322–328.

[16] Kaharudin KE, Salehuddin F, Zain ASM and Aziz MNIA. Optimization of Process Parameter Variations on Leakage Current in Silicon-on-insulator Vertical Double Gate Mosfet Device. Journal of Mechanical Engineering and Sciences. 2015;9:1614–1627.

[17] Afifah Maheran AH, Menon PS, Ahmad I, and Shaari S. Optimisation of Process

Parameters for Lower Leakage Current in 22 nm n-type MOSFET Device using Taguchi Method. Jurnal Teknologi. 2014;68(4):1–5.

[18] Kaharudin KE, Salehuddin F, Zain ASM and Aziz MNIA. Taguchi Modeling With The Interaction Test For Higher Drive Current in WSi_x/TiO_2 Channel Vertical Double Gate NMOS Device. Journal of Theoretical and Applied Information Technology. 2016; 90(1):185–193.

[19] Aziz MNIA, Salehuddin F, Zain ASM, Kaharudin KE, Hazura H, Idris SK, Hanim AR and Manap Z. Analyze of threshold voltage in SOI PMOSFET device using Taguchi method. IEEE International Conference on Semiconductor Electronics (ICSE), 2016;97–100.

[20] Faizah ZAN, Ahmad I, Ker PJ, Menon PS, and A. Meheran AH. V_{TH} and ILEAK Optimization Using Taguchi Method at 32nm Bilayer Graphene PMOS. Journal of Telecommunication, Electronic and Computer Engineering (JTEC). 2017;9(2):105–109.

[21] Othman NAF, Azhari FN, Hatta SFWM and Soin N. The Application of Taguchi Method on the Robust Optimization of p-FinFET Device Parameters. IEEE International Conference on Semiconductor Electronics (ICSE). 2016;141–144.

[22] Jamaluddin H, Jaharah AG, Deros BM, Nizam ARM, and Rizauddin R. Quality improvement using Taguchi method in shot blasting process. Journal of Mechanical Engineering and Sciences. 2016;10(2):2200–2213.

[23] Parate PR and Yarasu RB. Application of Taguchi and ANOVA in Optimization of Process Parameters of Lapping Operation for Cast Iron. Journal of Mechanical Engineering and Sciences. 2013;4:479–487.

[24] Prayogo GS and Lusi N. Application of Taguchi technique coupled with grey relational analysis for multiple performance characteristics optimization of EDM parameters on ST 42 steel. AIP Conference Proceedings, 2016;1725:020061-1-020061-7.

[25] Sekhar VC, Hussain SA, Pandurangadu V and Rao TS. Grey Relational Analysis to Determine Optimum Process Parameters of „ Emu ‟ Feather Fiber Reinforced Epoxy Composites. International Journal of Emerging Technology and Advanced Engineering. 2015;5(8):86–90.

[26] Nayak S and Routara BC. Optimization Of Multiple Performance Characteristics In Electro Discharge Machining Using Grey Relational Analysis. International Journal of Scientific & Technology Research. 2014;3(4):116–121.

[27] Sukhdeve V and Ganguly SK. Utility of Taguchi Based Grey Relational Analysis to optimize any Process or System. International Journal of Advanced Engineering Research and Studies. 2015;Jan-March:242–250.

[28] Shivapragash B, Chandrasekaran K, Parthasarathy C and Samuel M. Multiple Response Optimizations in Drilling Using Taguchi and Grey Relational Analysis. International Journal of Modern Engineering Research (IJMER). 2013;3(2):765–768.

[29] Lin HL. The use of the Taguchi method with grey relational analysis and a neural network to optimize a novel GMA welding process. Journal of Intelligent Manufacturing. 2012;23:1671–1680.

[30] Kaharudin KE, Salehuddin F, Zain ASM and Aziz MNIA. Application of Taguchi-based Grey Fuzzy Logic for Simultaneous Optimization in TiO_2/WSi_x-based Vertical double-gate MOSFET. Journal of Telecommunication, Electronic and Computer

Engineering. 2017;9(2–13):23–28.

[31] Kaharudin KE, Salehuddin F, Zain ASM, Aziz MNIA, Manap Z, Salam NAA and Saad WHM. Multi-response optimization in vertical double gate PMOS device using Taguchi method and grey relational analysis. IEEE International Conference on Semiconductor Electronics (ICSE). 2016;64–68.

[32] Kenghe KR and Patare PM. Optimization of Tribological Properties Using Grey Relational Analysis and Artificial Neural Network. International Engineering Research Journal. 2015;1(1):1022–1028.

[33] Kaharudin KE, Salehuddin F and Zain ASM. Optimization of Electrical Properties in TiO_2/WSi_x-based Vertical DG-MOSFET using Taguchi-based GRA with ANN. Journal of Telecommunication, Electronic and Computer Engineering. 2018;10(1):69–76.

[34] Noor CWM, Mamat R, Najafi G, Yasin MHM, Ihsan CK and Noor MM. Prediction of marine diesel engine performance by using artificial neural network model. Journal of Mechanical Engineering and Sciences. 2016;10(1):1917–1930.

[35] Chau R, Brask J, Datta S, Dewey G, Doczy M, Doyle B, Kavalieros J, Jin B, Metz M, Majumdar A and Radosavljevic M. Application of high-k gate dielectrics and metal gate electrodes to enable silicon and non-silicon logic nanotechnology. Microelectronic Engineering. 2015;80:1–6.

[36] Chau R, Datta S, Doczy M, Doyle B, Kavalieros J and Metz M. High-k/metal-gate stack and its MOSFET characteristics. IEEE Electron Device Letters. 2004;25(6):408–410.

[37] Silvaco. Silvaco ATLAS manual Device Simulation Software. 2006.